07177

Shear Strength Analysis of Ball Grid Array (BGA) Solder Interfaces

M. O. Alam, H. Lu and Chris Bailey *
School of Computing and Mathematical Sciences, University of Greenwich
30 Park Row, London SE10, 9LS, UK
* C.Bailey@gre.ac.uk
B. Y. Wu, and Y. C. Chan
Department of Electronic Engineering, City University of Hong Kong
83, Tat Chee Avenue, Kowloon Tong,
Hong Kong, China

Abstract:

Ball shear test is the most common test method used to assess the reliability of bond strength for ball grid array (BGA) packages. In this work, a combined experimental and numerical study was carried out to realize of BGA solder interface strength. Solder mask defined bond pads on the BGA substrate were used for BGA ball bonding. Different bond pad metallizations and solder alloys were used. Solid state aging at 150°C up to 1000 h has been carried out to change the interfacial microstructure. Cross-sectional studies of the solder-to-bond pad interfaces was conducted by scanning electron microscopy (SEM) equipped with an energy dispersive *X*-ray (EDX) analyzer to investigate the interfacial reaction phenomena. Ball shear tests have been carried out to obtain the mechanical strength of the solder joints and to correlate shear behaviour with the interfacial reaction products. An attempt has been taken to realize experimental findings by Finite Element Analysis (FEA). It was found that intermetallic compound (IMC) formation at the solder interface plays an important role in the BGA solder bond strength. By changing the morphology and the microchemistry of IMCs, the fracture propagation path could be changed and hence, reliability could be improved.

Introduction:

In Ball Grid Array (BGA) packages, area-array soldering technology is used through an interposer to attach to the Printed Circuits Board (PCB). By the virtue of area-array distribution, BGA interconnections on a PCB generally consist of relatively high numbers of solder joints per device in comparison with other electronic packages [1-2]. However, array solder interconnections are less compliant than conventional peripheral-leaded interconnections. The decreased compliance contributes high stress concentrations at the solder interfaces that may arise during bending, vibration, thermal fatigue etc. If any one of these solder joints fails, there is a chance that the whole package malfunctions. Usually, there is provision for redundancy in packages with critical solder balls but nonetheless, reliability of every one of these solder joints is important for the overall function of a package which in turn is related to interfacial reactions between the solder alloy and the soldering pad (such as a BGA bond pad). The solder ball shear test and solder ball pull test have been used to evaluate the reliability of area-array solder joint such as for BGA packages where as ball shear test is used as a standard qualification test. In July of 2000, JEDEC established a standard for solder ball shear test for BGA solder joint, JESD22-B117. The stated purpose of this test is to determine the ability of the BGA to withstand mechanical shear forces that may be applied during module manufacturing and handling operations. The test applies to shear force testing of the solder balls on the BGA, prior to second level attachment to the PWB.

The tri-layer metallization of Au/Ni/Cu is a popular choice for BGA bond pads. The outermost Au-layer serves to protect the UBM/pad from corrosion and oxidation as well as to increase solderability. The Ni layer serves the purpose of a diffusion barrier to inhibit the out-diffusion of Cu to the Au-protective layer during storage time and to prevent the rapid consumption of the Cu layer [3-6]. The Au coating (usually 0.1-1 μm) dissolves very quickly into the molten solder during reflow and precipitates as intermetallic compound (IMC) of $AuSn_4$ in the matrix of the solder upon cooling while the Ni reacts with Sn to form a thin Ni_3Sn_4 intermetallic layer at the interface. However, it is surprising that after the package is subjected to several hundred hours of solid-state aging at 100-150°C, most of these $AuSn_4$ needle-like precipitates migrate to the Ni interface and form a continuous layer of $(Au,Ni)Sn_4$ over the Ni_3Sn_4 layer [6-9]. The aged joints were found to be significantly weaker than the same joints tested before aging. The redeposition of the $(Au,Ni)Sn_4$ as a continuous layer degrades the strength and ductility of the solder/pad interface, eventually resulting in Au-embrittlement of the solder interconnection. This $(Au,Ni)Sn_4$ ternary intermetallic (TIMC) was reported to grow at a rather faster rate than the binary intermetallic (BIMC) during the aging treatment [10].

It is now confirm that the utilization of a Ni layer in between Au and Cu, makes solder interface susceptible to the Au-embrittlement. On the other hand, the Ni is required to protect Cu UBM at least up to reflow soldering. Hence, it is timely to compromise these two opposite requirements by optimizing Ni layer thickness just enough to survive up to reflow soldering. This work is attempted to study the relationship of the effect of Ni layer thickness on the mechanical strength of the solder joint and the underlying mechanism of the complex TIMC formation at the solder interface. Numerical modeling is being carried out to understand deformation and fracture behavior in terms of microstructure modeling.

Experimental Procedures:

A solder mask-defined bare Cu bond pad on a BGA substrate was used as a base for electrodeposition of Au and Ni. The thickness of the Ni layer was varied from 0.35 μm to 2.8 μm. The thickness of Au was varied from 0.1 μm to 1.3 μm. Commercially-available BGA solder balls of Sn-

36wt.%Pb-2%Ag were used for this study. The solder mask-opening diameter was 600 μm and the diameter of the BGA solder ball before melting was 760 μm. Solder balls were placed on the pre-fluxed Au/Ni/Cu bond pads and reflowed in a N_2 atmosphere reflow oven. The peak reflow temperature was 225°C and the time above the melting point of the solder alloy was 30 s on one line. Immediately after the reflow, the substrates were subjected to aging at 150°C for times up to 1000 h. After the aging test for each readout point, one set of substrates was used for mechanical testing and the other set for cross-sectional studies. The mechanical strength of the interface was measured by performing a typical shear test using the Dage Series 4000 Bond Tester. Figure 1 shows a schematic diagram of the shear test configuration used in testing the BGA solder joints. The shear height and the test speed of the shear test in this work were about 100 μm and 550 μm/s respectively. Forty randomly chosen solder balls were sheared to obtain the average interfacial strength. The cross-sectioned samples were prepared to study interfacial microstructure. After the shear tests, fracture surfaces have also been investigated to understand the fracture modes. The Scanning Electron Microscope (SEM) used for this study was a Philips XL 40 FEG that is equipped with energy dispersive x-ray analysis (EDX) facility.

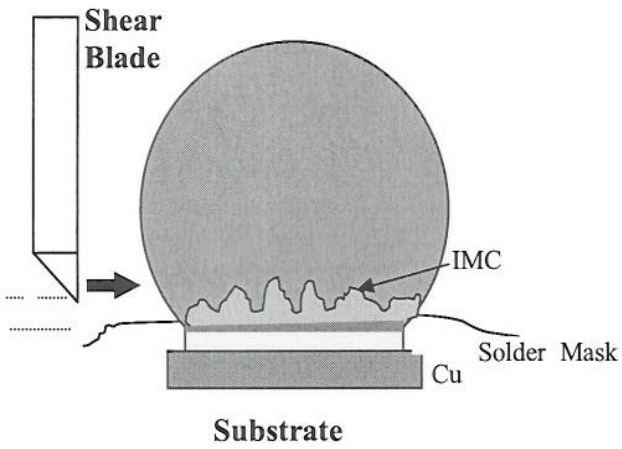

Figure 1: Schematic diagram of the shear test configuration for a BGA solder joint.

Experimental Results:

Figure 2 shows the change of average interfacial strength of the solder joint along with the aging time at 150°C for each Ni layer when the Au layer was kept 1.3 μm thick. From the curves, it is clear that during early stage of aging time, all the layers showed decreasing trend in the interfacial strength. However, for thinner Ni layers, interfacial strength decreased at a lesser extent. At 100 h, interfacial strength increased instead, which is significant for the thinnest Ni layer. For the case of two thinner Ni layers, solder joint strength did not fall below the 1 Kgmf, which is the minimum requirement for a BGA solder ball of 760 μm diameter. The significant finding of this work is to obtain higher interfacial strength for the thin Ni layer.

The significant finding here is that to maintain higher interfacial strength for bond pad having a thick Au layer, a thin Ni layer is needed. The reason for such an unusual finding is explained through an in-depth study of their fracture surfaces as well as their microchemistry and interfacial microstructure. After measuring the interfacial strength, fractured surfaces of the residue pads and sheared balls were studied immediately under an SEM. The fracture surfaces of solder joints for the samples with a thin Au layer (0.1μm thick) showed a ductile mode irrespective of the Ni layer thickness. Figure 3 shows typical fracture surfaces of the solder balls for the sample of a thin Au layer aged for 500h at 150°C. From the fractograph, it is clear that this kind of joint fails in a ductile mode. From EDX analysis, it was also confirmed that the fracture occurred through the solder joint.

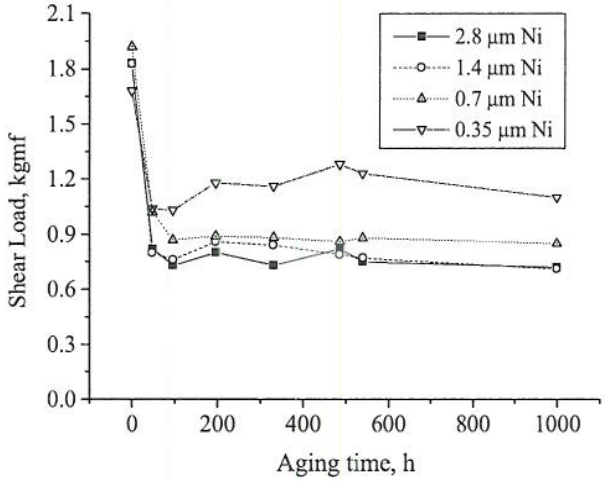

Figure 2: Interfacial shear load of solder joints with pads having a thick Au layer as a function of the aging time at 150°C.

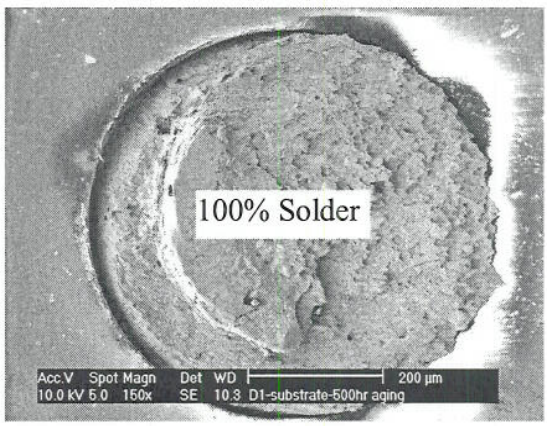

Figure 3: Typical fracture surfaces of the solder joint (substrate pad side) for a thin Au layer (0.1 μm) aged for 500h at 150°C.

Figure 4 shows the fracture surfaces of solder balls and the corresponding substrate pads for a 1.3 -μm-Au and 2.8-μm-thick Ni layer aged for 500 h at 150°C. From the fractograph, it is clear that the interface fails in a brittle mode through the IMC layer. By EDX analysis, it is confirmed that fracture occurred through the interface between $(Au,Ni)Sn_4$ layer and Ni_3Sn_4 layer. On the other hand, the solder joint of the sample

with a 1.3 -μm-Au and 0.35-μm-thick Ni layer showed a peculiar fracture mode (see Figure 5). The fracture surface on the solder ball side showed smearing of the solder alloy—typical of a ductile mode, whereas, at the bond pad side, no evidence of a ductile mode is revealed. From the EDX analysis and fracture morphology, it is confirmed that fracture occurred at the solder/IMC interface. This is why the solder alloy on the ball side experienced some deformation, whereas the IMC at the pad side did not show any ductility. In some locations on the pad side, residual solder and fractured $AuSn_4$ IMC were detected; most of the remaining IMCs were quaternary IMC of Au, Ni, Cu, and Sn.

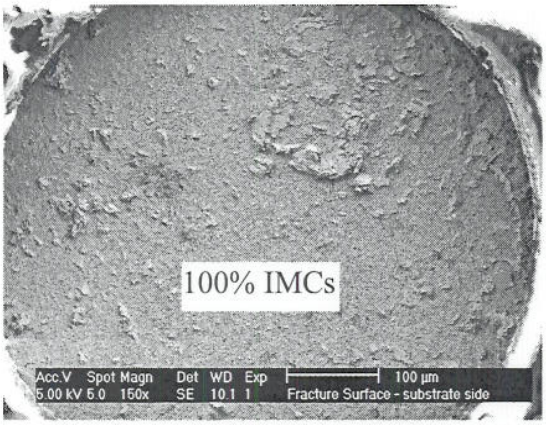

Figure 4: Fracture surface of the solder joint (substrate pad sided) for a 2.8 μm thick Ni and a 1.3 μm thick Au layer aged for 500h at 150°C.

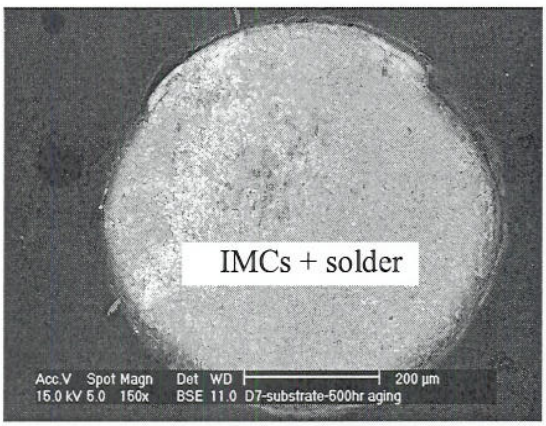

Figure 5: Fracture surface of the solder joint (substrate pad sided) for a 0.35 μm thick Ni and a 1.3 μm thick Au layer aged for 500 h at 150°C.

Figure 6 shows the interfacial microstructure of a solder joint after 500h of aging at 150°C for (a) a thick Ni layer and (b) a thin Ni layer with a thick Au layer. A new layer of $(Au,Ni)Sn_4$ nucleated and grew on the Ni_3Sn_4 IMC layer in the sample having a thick Au and a thick Ni layer. Many other investigators have reported the same interfacial structures [7-11]. As aging progresses, both $(Au,Ni)Sn_4$ and Ni_3Sn_4 grew thicker by taking Sn atoms from the solder neighboring the interface. As a consequence, a continuous Pb-rich layer forms adjacent to the $(Au,Ni)Sn_4$ layer. On the other hand, the interfacial structure for a thin Ni layer, shown in Figure 6 b, is totally different from that with a thick Ni layer. Here, there is no $(Au,Ni)Sn_4$ layer. The chemistry and morphology of the interfacial IMC is very different from that of the thick Ni metallization. Due to Cu diffusion, the layer-type morphology of $(Au,Ni)Sn_4$ no longer exists; instead, $AuSn_4$ is detected with a spherical morphology. Underneath the $AuSn_4$ spheres, a complex quaternary $(Au,Ni,Cu)_6Sn_5$ IMC is detected. This is a new finding and helps in the understanding of the reason for higher interfacial strength in the case of a thin Ni metallization even when a thick Au layer is used on the BGA solder ball pad.

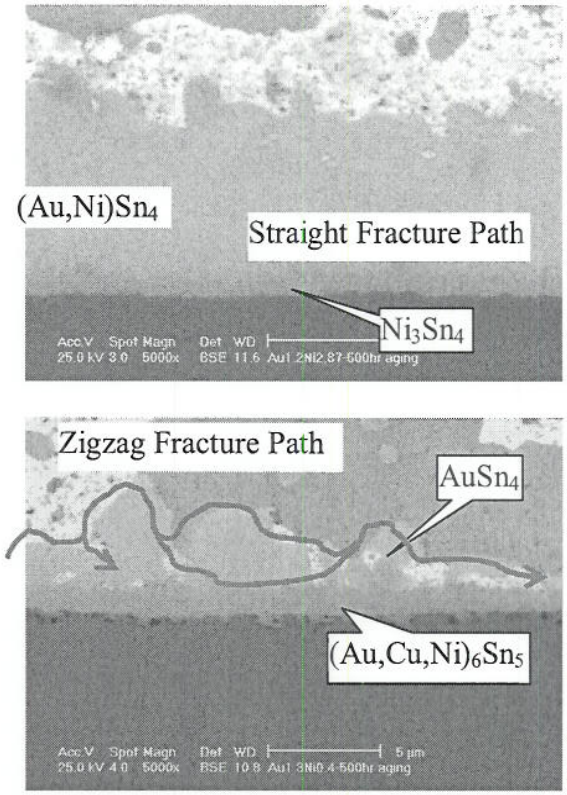

Figure 6: Interfacial structure of the solder/bond pad interfaces after 500h of aging at 150°C for a thick Ni layer (a) and a thin Ni layer (b).

Finite Element Analysis:

To understand the experimental findings, finite element analysis (FEA) has been carried out. FEA reported herein is from the early stage of research. At the first phase, we tried to understand deformation behaviour of solder joint during shear test. A comparative study was carried out with the variation of IMC morphology at the solder interface.

Table I and Table II lists the materials properties of the components of BGA solder joint that are used in the FEA. While all the materials are assumed to be linear elastic, solder ball is considered to be elasto-plastic. The contact behaviour between the solder ball and the shear ram has been simulated using 2-D contact element (CONTA172) and surface to surface target element (TARGE169). The CONTA172 element is applied to the surface of solder ball and the TARGE169 element is applied to the surface of shear ram. The shear ram is considered 1000 times stiffer than the solder. To ensure full convergence, the full Newton-Raphson method with a sub-step iteration was used.

Table I Linear elastic materials properties for BGA solder joint

Materials	Young's Modulus (GPa)	Poisson Ratio
Solder	28.9	0.40
Cu	128.7	0.34
BGA Substrate	14	0.39
Shear Ram	29.8 X 1000	0.33
IMC	112	0.31

Table 2 Multilinear isotropic hardening materials parameters for 62Sn36Pb2Ag [12]

Stress, MPa	35	46	48
Plastic Strain	0.0011	0.0211	0.0411

Figure 7 shows the distribution of plastic equivalent stress in the solder ball without IMC (a), with layer-typed IMC (b) and with nodular-typed IMC when shear ram moves a displacement of 20 micron in contact with the solder ball.

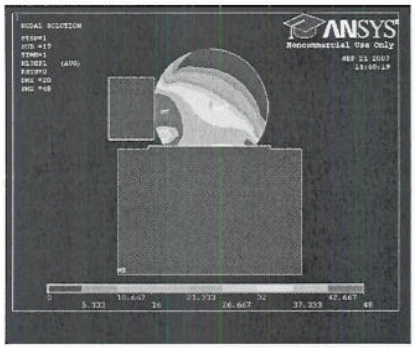

(a) Plastic Equivalent Stress in the solder ball without IMC

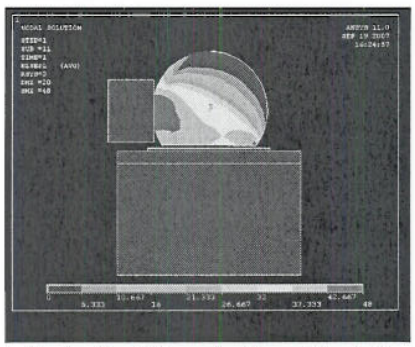

(b) Plastic Equivalent Stress in the solder ball with layer-typed IMC

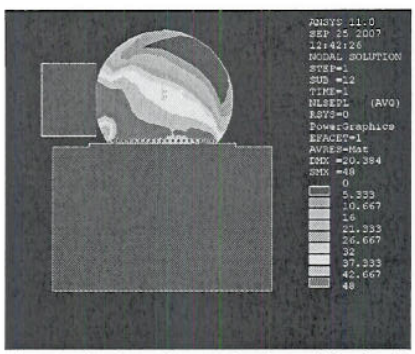

(c) Plastic Equivalent Stress in the solder ball with nodular-typed IMC

Figure 7: Distribution of averaged plastic stress in the solder ball after 20 mm displacement of shear ram.

Conclusion:

During aging at 150°C, the thin Ni layer facilitates Cu diffusion from the bond pad towards IMCs. As a result, the brittle continuous layer of $(Au,Ni)Sn_4$ and Ni_3Sn_4 are transformed into a nodular-shaped discontinuous layer of $AuSn_4$ and a layer of $(Au,Cu,Ni)_6Sn_5$ respectively. New interfacial reaction products with the modified morphology change the typical scenario of Au-embrittlement at the BGA solder interface and thus improve the interfacial joint strength significantly. Although it is an early state of numerical modeling research, it can be seen that IMC morphology changes stress-strain characteristics at the solder interface.

Acknowledgments

The authors from the University of Greenwich, UK would like to acknowledge the EU funded Marie Curie Incoming International Fellowship project MIFICT-2006-022113.

References:

1. J. H. Lau, *Ball grid array technology*, McGraw-Hill, New York, 1995.
2. K. Gilleo, *Area array package design : techniques in high-density electronics*, McGraw-Hill, New York : London, 2004.
3. M. O. Alam and Y. C. Chan, "Interfacial reaction phenomena of Sn-Pb solder with Au/Ni/Cu metallization", ACS journal, Chemistry of Materials, volume 17, issue 5, pp 927 – 930, March 2005.
4. M. O. Alam and Y. C. Chan, "Solid State Growth Kinetics of Ni_3Sn_4 at the Sn-3.5Ag Solder/Ni Interface" Journal of Applied Physics, 98 (12): pp. 123527:1-4, DEC 15 2005,.
5. M. O. Alam, Y. C. Chan and K. N. Tu, "Effect of 0.5 wt.% Cu in Sn-3.5%Ag solder on the interfacial reaction with the Au/Ni metallization", ACS journal, Chemistry of Materials, 15(23), pp. 4340-4342, 2003.
6. M. O. Alam, Y. C. Chan and K. N. Tu, "Elimination of Au-embrittlement in solder joints on Au/Ni metallization", Journal of Materials Research, 19(5), pp. 1303-1306, 2004.
7. A. Zribi, "*Kinetics of intermetallic growth at the interfaces of soldered metallizations*", Ph.D. Thesis, State University of New York at Binghamton, 2002.
8. C. E. Ho, S. Y. Tsai, C. R. Kao, "Reaction of solder with Ni/Au metallization for electronic packages during reflow soldering", IEEE Transactions on Advanced Packaging, 24 (4), pp. 493-498, 2001.
9. P. G. Kim and K.N. Tu, "Fast dissolution and soldering reactions on Au foils", Materials Chemistry and Physics, 53(2), pp. 165–171, 1998.
10. A. M. Minor, "*Growth of a Au-Ni-Sn intermetallic compound on the solder-substrate interface after aging*", M. S. Thesis, University of California, Berkeley, 1999.
11. C. E. Ho, R. Zheng, G.L. Luo, A.H. Lin and C.R. Kao, "Formation and resettlement of $(Au_xSn_{1-x})Sn_4$ in solder joints of ball–grid-array packages with the Au/Ni surface finish", Journal of Electronic Materials, 29 10 (2000), pp. 1175–1181
12. S. C. Tseng, R. S. Chen and C. C. Lio, "Stress analysis of lead-free solders with under bump metallurgy in a wafer level chip level package", Int J Adv Manuf Technol, 31, pp. 1-9, 2006.